10.1071/WR22072

Wildlife Research

Supplementary Material

Factors affecting recent population decline and range contraction of the greater long-tailed hamster in China

Da Zhang[A,B], *Xinru Wan*[A], *Defeng Bai*[A,B], *Zhenyu Wang*[C], *Yongwang Guo*[D], *and Zhibin Zhang*[A,E,*]

[A]State Key Laboratory of Integrated Management of Pest Insects and Rodents, Institute of Zoology, Chinese of Academy of Sciences, Beijing 100101, China.

[B]University of Chinese Academy of Sciences, Beijing 100049, China.

[C]Key Laboratory of Poyang Lake Wetland and Watershed Research (Ministry of Education), College of Life Sciences, Jiangxi Normal University, Nanchang 330027, China.

[D]National Agro-tech Extension and Service Center, Ministry of Agriculture, Beijing 100125, China.

[E]CAS Center for Excellence in Biotic Interactions, University of Chinese Academy of Sciences, Beijing 100049, China.

[*]Correspondence to: Zhibin Zhang State Key Laboratory of Integrated Management of Pest Insects and Rodents, Institute of Zoology, Chinese of Academy of Sciences, Beijing 100101, China Email: zhangzb@ioz.ac.cn

Supporting information

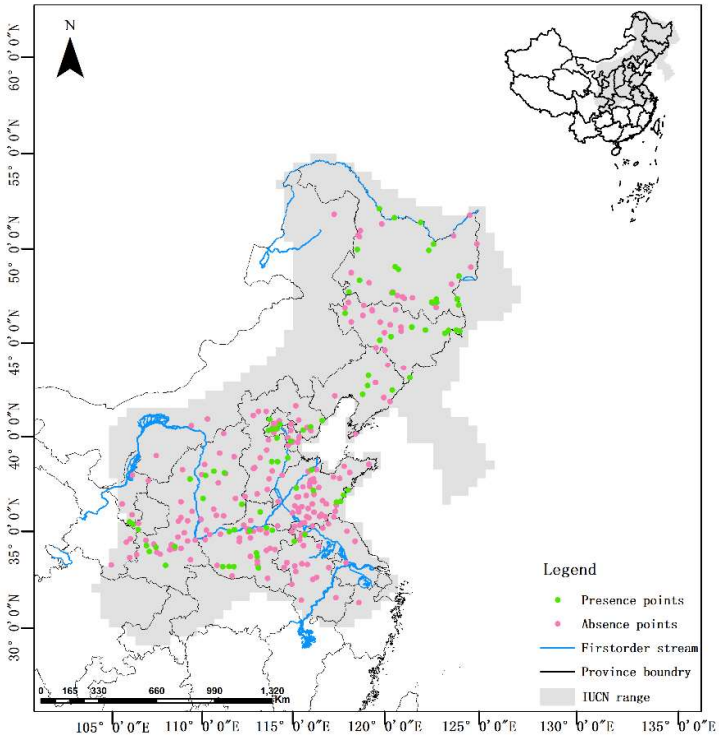

Fig. S1 Presence (green points) and absence (pink points) data of the greater long-tailed hamster in China by 2017. The last observation time of the grid is defined based on the survey conducted by the Ministry of Agriculture and Rural Affairs of China during 2008–2012 and the literature that the records year after 2008. The grey shaded area represents the geographic range of greater long-tailed hamster in the IUCN global assessment (last assessed 18 August 2016, version 2021-1).

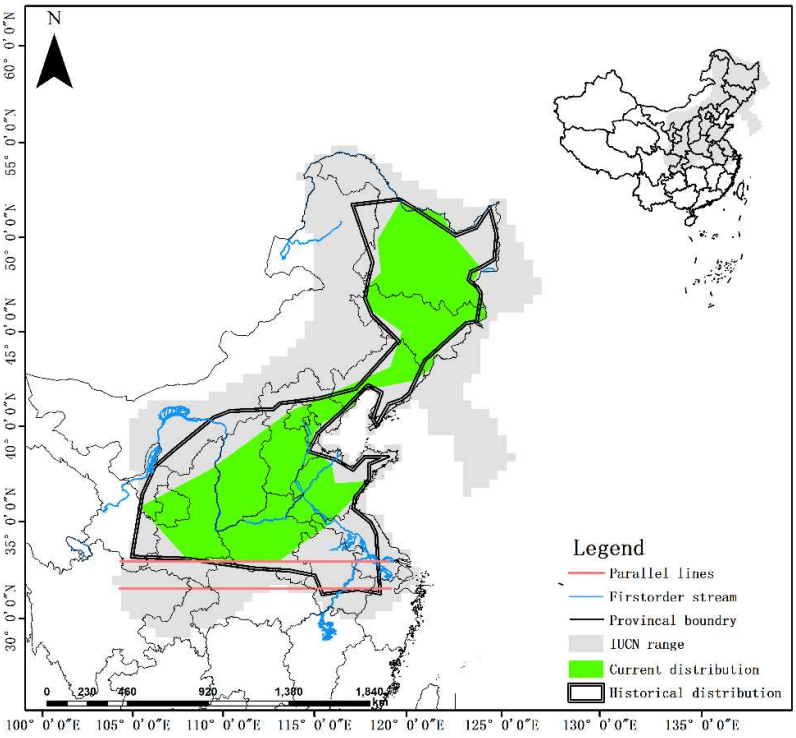

Fig. S2 The historical distribution and current distribution of the greater long-tailed hamster in China. The grey shaded area represents the geographic range of the greater long-tailed hamster in the IUCN global assessment (last assessed 18 August 2016, version 2021-1). We measured the distance of parallel lines between the edge of the past distribution area and the edge of the current distribution area as the contraction distance.

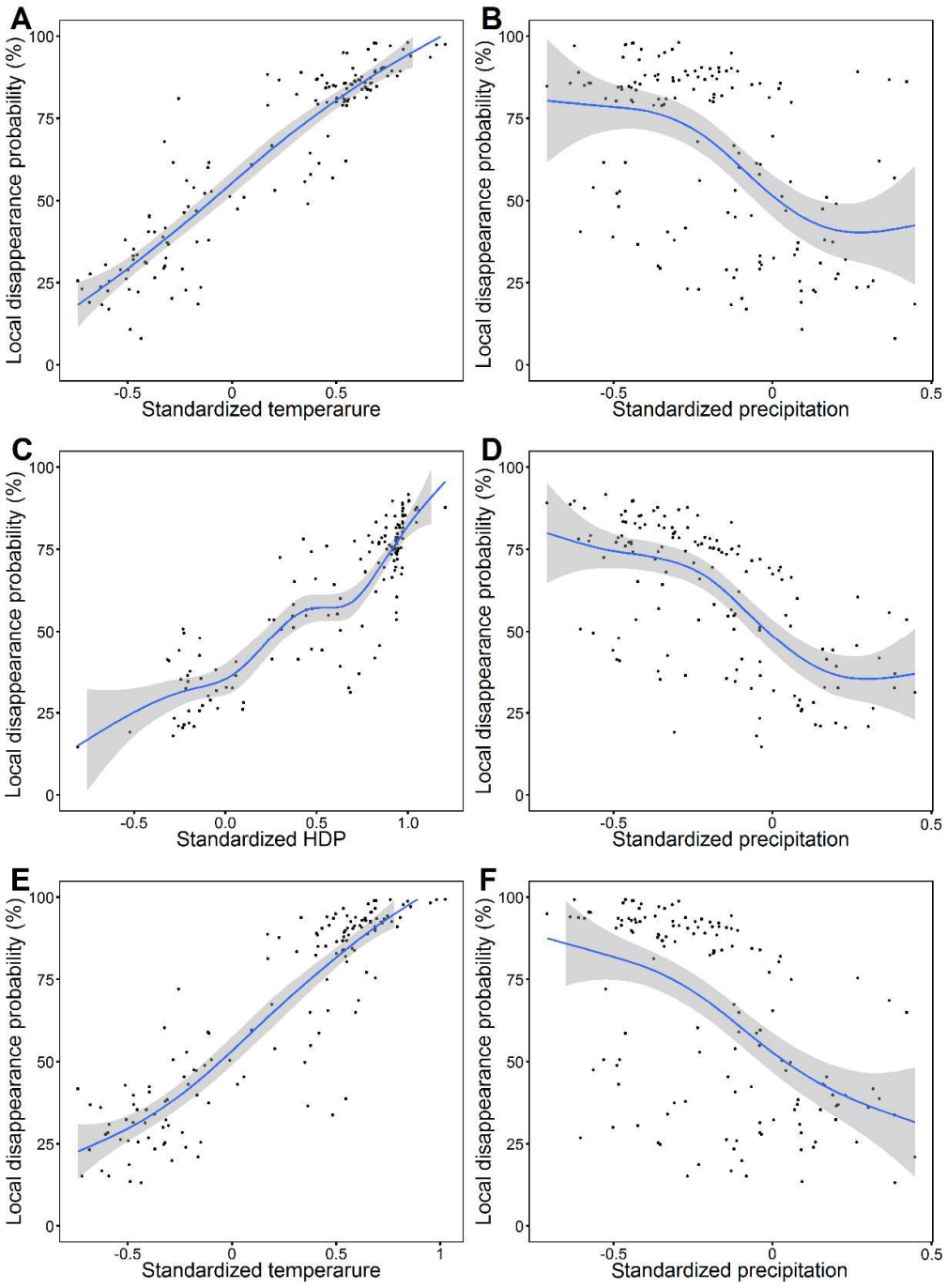

Fig. S3 Relationship between the local disappearance probability of the greater long-tailed hamster and the standardized temperature, standardized human population density and standardized precipitation excluding interactive effects (Eqn 3: A–B and Eqn 4: C–D) and including interactive effects (Eqn 5: E–F). The average local disappearance probability for precipitation and temperature or human population density was estimated using the standardized coordinates of each grid in Eqn 3 and Eqn 4, and the interaction effect between temperature and precipitation used Eqn 5.

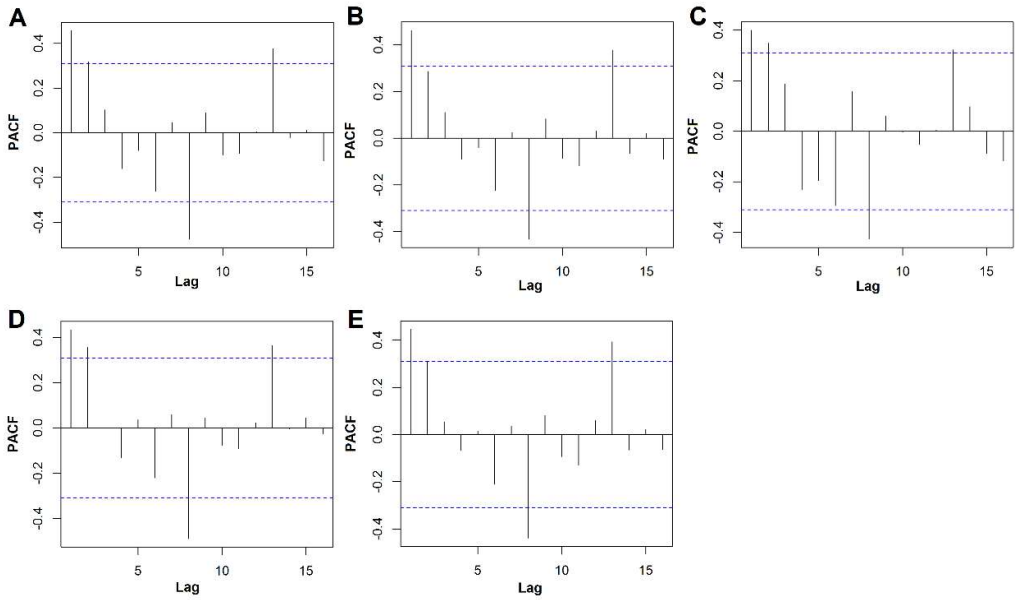

Fig. S4. Partial autocorrelation function (PACF) of the yearly averages of the residuals diagnostics for the greater long-tailed hamster. A: PACF excluding interactive effects (temperature, precipitation and human population density); B: PACF excluding interactive effects (temperature and precipitation); C: PACF excluding interactive effects (human population density and precipitation); D: PACF including interactive effects (interaction effects between temperature, precipitation and human population density). E: PACF including interactive effects (temperature, precipitation, and their interactive effects). The dashed horizontal lines reveal confidence intervals of PACF. Due to the short disappearance interval, a little residual autocorrelation was detected above here, indicating that the model result is still acceptable.

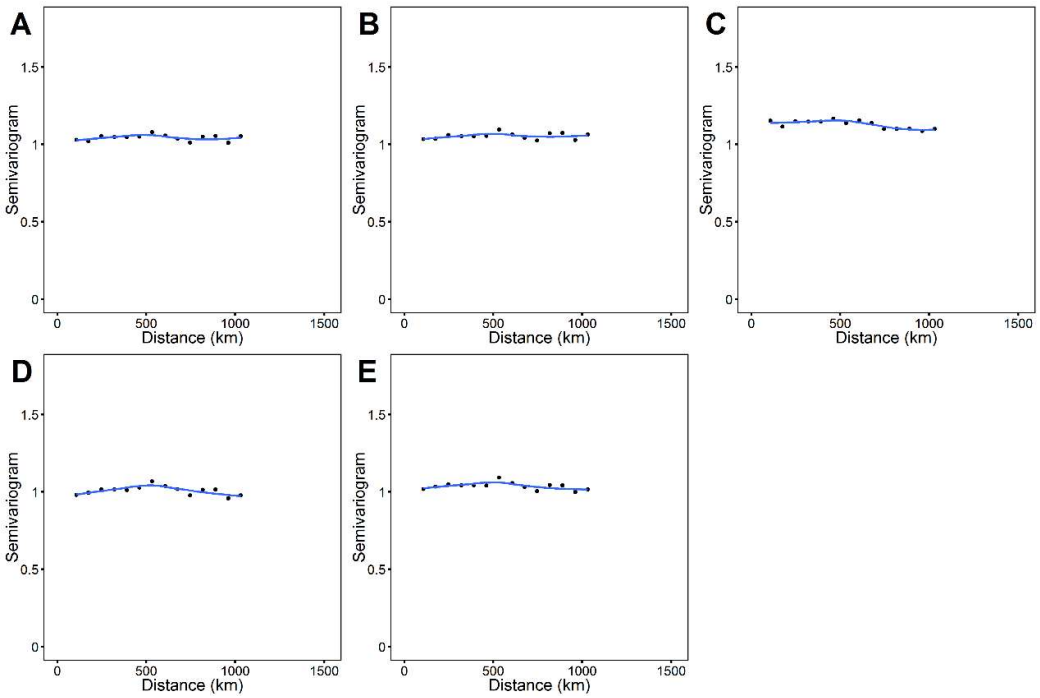

Fig. S5. Residual semivariogram diagnostics of the spatial correlation in the residuals for the greater long-tailed hamster. A: semivariogram excluding interactive effects (temperature, precipitation and human population density); B: semivariogram excluding interactive effects (temperature and precipitation); C: semivariogram excluding interactive effects (human population density and precipitation); D: semivariogram including interactive effects (interaction effects between temperature, precipitation and human population density); E: semivariogram including interactive effects (temperature, precipitation, and their interactive effects). The semivariogram curves were approximately flat suggesting there was little remaining residual spatial autocorrelation for the greater long-tailed hamster.

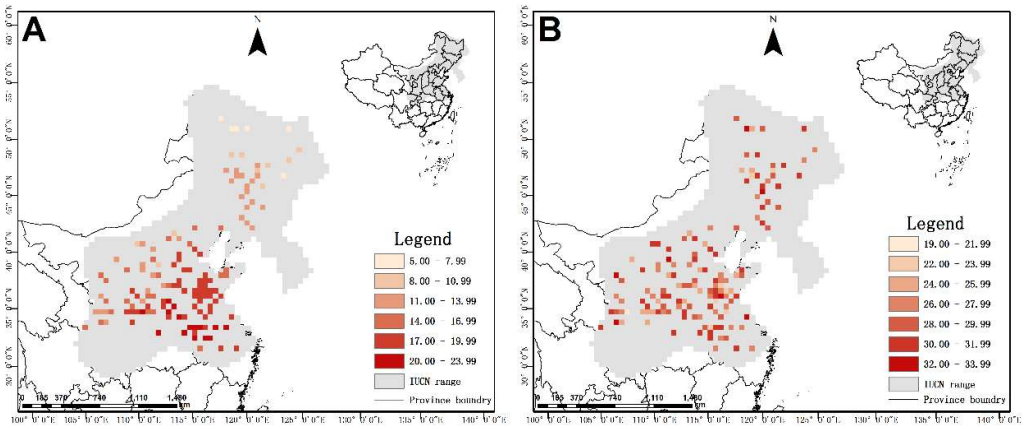

Fig. S6. A: Yearly maximum air temperature and B: average maximum air temperature of the warmest months (from June to August) in the disappearance year in each grid used for the greater long-tailed hamster. The disappearance year was defined as the first year after the last observation time of each grid. The disappearance threshold of the yearly maximum temperature and average maximum air temperature of the warmest months was 15.8 ± 3.87 °C and 28.21 ± 2.71 °C, respectively. The grey shaded area represents the geographic range of the greater long-tailed hamster in the IUCN global assessment (last assessed 18 August 2016, version 2021-1). Darker red indicates higher temperatures in the disappearance year.

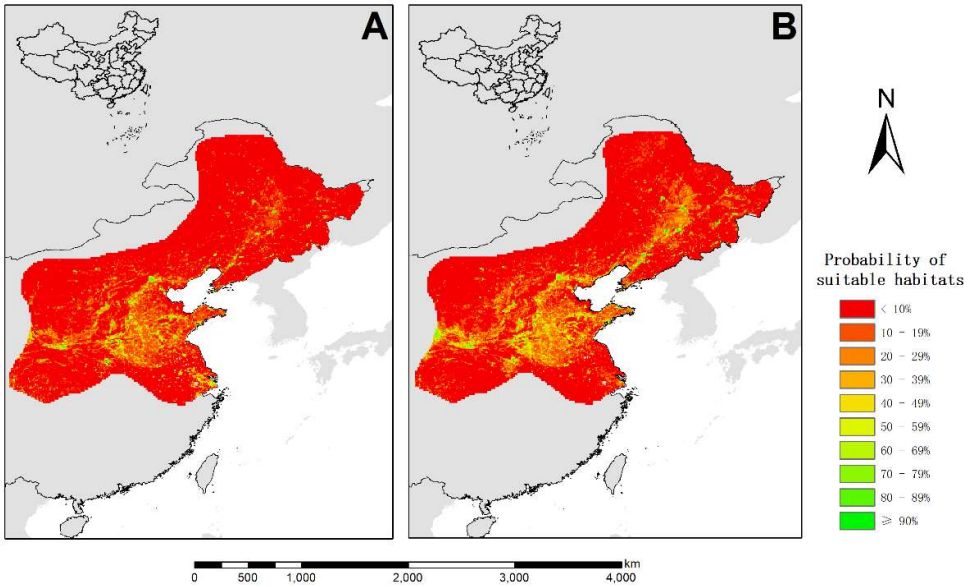

Fig. S7. The MaxEnt method of species distribution models (SDMs) was used to project changes in suitable habitat for the greater long-tailed hamsters using the presence-only data and environment data. A and B represent suitable habitats in the past (1961–2008) and current (2009–2018), respectively. The predicted probabilities of the suitable habitats were represented by color (red to green: low to high).

Table S1 Verification of the historical distribution data of the greater long-tailed hamsters in China. A total of 5809 records of the greater long-tailed hamster were collected, including 2494 records of absence (Investigated but the capture success rate is 0). After removing the data that does not conform to the data type, only the presence data of the greater long-tailed hamster with specific year or location was used for statistical analysis, and finally 3178 records are used.

	Data classification	Data type	Data description	Number of records	Usage
Description	A	All records	" greater long-tailed hamster ", "*Tscherskia triton*", "*da cang shu* (in Chinese)", description records in historical literatures.	5809	Included
	B	Absence	Investigated but the capture success rate is 0	2494	Excluded
	C	Unclear	Latin name of species confusion	12	Excluded
Spatial	A	Specific Location	Presence locations with latitude and longitude or specific location description (e.g., 42°45′ N,130°35′ E or village)	3303	Included
	B	Provincial and municipal	Presence information with only provincial and municipal description (e.g., Henan province or Baoji, Shanxi province)	45	Excluded
	C	Out of boundary	Out the boundary of IUCN	20	Excluded
	D	Unclear	Without specific spatial description	4	Excluded
Time	A	Year	Specific sampling year	3178	Finally Included
	B	Decade	Not designated to specific year but within one decade (e.g., the 1980s)	49	Excluded
	C	Unclear	Without specific time information for sampling	7	Excluded

Table S2 Correlation analysis between independent variables. *** $p < 0.001$.

	Standardized human population density	Standardized precipitation	Standardized temperature
Standardized human population density	1	-0.23***	0.74***
Standardized precipitation	-0.23***	1	-0.37***
Standardized temperature	0.74***	-0.37***	1

Table S3 Correlation between survival rates (proportion of survived grids) of the greater long-tailed hamsters (ratio of survival grid points) and temperature, population density, and precipitation. The grid resolution is 0.5° × 0.5°. *** $p < 0.001$.

	Correlation coefficients		
	Temperature	Human population density	Precipitation
Survival rate of the greater long-tailed hamster	-0.56	**-1*****	0.22

Table S4 Model selection with interactions between variables. T_{it}, P_{it}, and H_{it} represent standardized temperature, standardized precipitation, and standardized human population density, respectively. The model only chooses to select significant interaction effects. s(Latitude, Longitude, k=4) is the spatial autocorrelation effects. All models were ranked by smaller value of unbiased risk estimators (UBRE).

Model	Deviance explained	R^2	UBRE	AIC
Models with significant interactive effects				
$Y_{it} \sim T_{it} + P_{it} + T_{it}:P_{it} + s(Lon_i, Lat_i)$	25.5%	0.275	0.08000	308.8802
$Y_{it} \sim T_{it} + H_{it} + P_{it} + T_{it}:H_{it} + T_{it}:P_{it} + P_{it}:H_{it} + s(Lon_i, Lat_i)$	27%	0.280	0.07963	308.7734
Models without interactive effects				
$Y_{it} \sim T_{it} + H_{it} + P_{it} + s(Lon_i, Lat_i)$	24.5%	0.265	0.09368	312.7922
$Y_{it} \sim T_{it} + P_{it} + s(Lon_i, Lat_i)$	23.9%	0.266	0.09518	313.2226
$Y_{it} \sim H_{it} + P_{it} + s(Lon_i, Lat_i)$	17.7%	0.197	0.17744	336.7482

Table S5 Number of grids with disappearance temperature threshold of yearly maximum air temperature and average maximum temperature of the warmest months (from June to August) for the greater long-tailed hamster in the first disappearance year. The disappearance year was defined as the first year after the last observation time in each grid. The disappearance temperature threshold of the yearly maximum temperature and average maximum air temperature of the warmest months was 15.8 ± 3.87 °C and 28.21 ± 2.71 °C, respectively.

Yearly maximum air temperature range (°C)	Number of grids	Maximum temperature of the warmest month (°C)	Number of grids
5.00–7.99	6	19.00–21.99	1
8.00–10.99	10	22.00–23.99	8
11.00–13.99	33	24.00–25.99	21
14.00–16.99	25	26.00–27.99	33
17.00–19.99	52	28.00–29.99	27
20.00–23.99	15	30.00–31.99	46
		32.00–33.99	5